Report on "Self-directed Joint Research" of MERIT program

Sulfur-doped Finite Carbon Nanotube Molecules: Design, Synthesis and Properties

Chizuru Sawabe[1], Toshiya Fukunaga[2]

[1]Department of Advanced Materials Science, Graduate School of Frontier Sciences, Takeya & Okamoto & Watanabe Lab

[2]Department of Chemistry, Graduate School of Science, Isobe Lab.

Abstract

The dissymmetry factor *g* in circular dichroism and circularly polarized luminescence is governed by magnetic and electric transition dipole moments (***m*** and ***μ***) and maximized to 2 when ***m***∥***μ*** and |***m***|=|***μ***|. Chiral nanotube molecules were already found to satisfy ***m***∥***μ*** and be suitable for enhancing *g*. In this study, a chiral nanotube was desymmetrized by doping sulfur atoms to balance ***m*** and ***μ*** (|***m***|~|***μ***|). Although desymmetrization succeeded in balancing the two moments, *g* value was failed to be maximized. Structural studies suggested *g* value is sensitive to the structural fluctuations in the solution.

Authors

Chizuru Sawabe is engaging in development of organic semiconductor materials. In this study, C. Sawabe is responsible for the synthesis of target molecules and the examination of the performance as organic semiconductors.

Toshiya Fukunaga is engaging in the research of physical organic chemistry in nanocarbon molecules. In this study, T. Fukunaga is responsible for the synthesis of target molecules and the examination of the performance as chiroptical materials.

Introduction

Circular dichroism (CD) and circularly polarized luminescence (CPL) are fundamental properties of chiral molecules.[1,2] These properties are given by biases in interactions with polarized electromagnetic waves and chiroptical properties of chiral molecules are extensively being investigated. The difference of intensity for polarized light in CD and CPL is represented as the dissymmetry factor *g*, which is governed by

magnetic and electric transition dipole moments (***m*** and ***μ***) and maximized to 2 if ***m*** ∥ ***μ*** and |***m***|=|***μ***|. Though the dissymmetry factors *g* for organic compounds have remained around 10^{-3} so far[3], a chiral nanotube molecule (*P*)-(12,8)-[4]cyclochrysenylene (**[4]CC**) was found to show the highest dissymmetry factors to date.[4] Theoretical calculations revealed that two elements, curve π-systems aligned circularly gives a large ***m*** and ***m*** is parallel to ***μ*** with an angle θ of 0° or 180°, are important for enhancing |*g*| values (Figure 1). The structure-property relationship of chiral nanotube molecules have not been studied and the determinant factors for maximizing |*g*| values are still unknown.[5] Here, we attempted to maximize |*g*| values with the molecular design of sulfur doping into nanotube structures. A desymmetrization strategy by sulfur doping have been devised to manipulate the chiroptical properties.

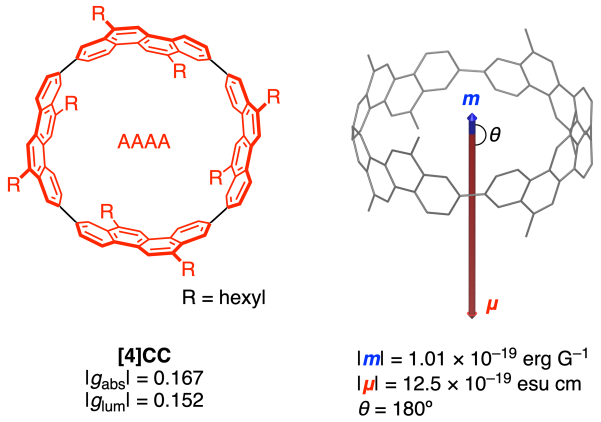

Figure 1. A chiral nanotube molecule with the highest |*g*| values. Arrows for moments are displayed with 1×10^{-19} erg G^{-1} = 1 Å for ***m*** and 1×10^{-19} esu cm = 1 Å for ***μ***.

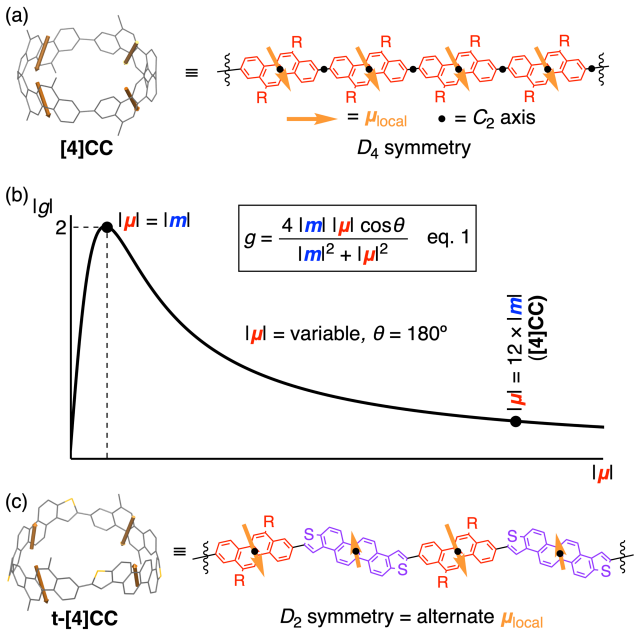

Figure 2. Desymmetrization strategy to achieve high |*g*| values in chiral nanotubes. (a) Decomposition analyses of ***μ*** in **[4]CC**. (b) A |***μ***|-|g| plot with ***m*** ∥ ***μ***. (c) Decomposition analyses of ***μ*** in **t-[4]CC**.

Results & Discussion

-Molecular Design

In the molecular design for enhancing |*g*| values of chiral nanotube molecules, we focused on the balance of ***m*** and ***μ***. The total ***μ*** can be decomposed into the local contributions $\boldsymbol{\mu}_{\text{local}}$ of four arylene panels (Figure 2a).[4,6] In **[4]CC**, the directions of $\boldsymbol{\mu}_{\text{local}}$ of four panels are the same because the molecule has D_4 point group symmetry and is composed of four same arylene panels in the identical directions. As a result of adding up $\boldsymbol{\mu}_{\text{local}}$ vectors with same directions, ***μ*** in **[4]CC** is much larger than ***m*** (|***m***|<|***μ***|). If the |***μ***| value was reduced to satisfy the relationship |***m***|=|***μ***|, the |*g*| value can be expected to reach its theoretical maximum 2 (Figure 2b). Therefore, we thought that doping heteroatoms in panels can manipulate the local contributions $\boldsymbol{\mu}_{\text{local}}$ to reduce ***μ*** and designed thiopheno-doped [4]CC (**t-[4]CC**) (Figure 2c). Desymmetrization induced by the introduction of two different arylene panels makes the symmetry down to D_2, and introduces alternate and antiparallel $\boldsymbol{\mu}_{\text{local}}$. According to the theoretical calculations, an ideal relationship of |***m***|~|***μ***| is achieved with this thiopheno-doped structure at the global minimum, and the large |*g*| value of 1.67 was predicted (Figure 3).

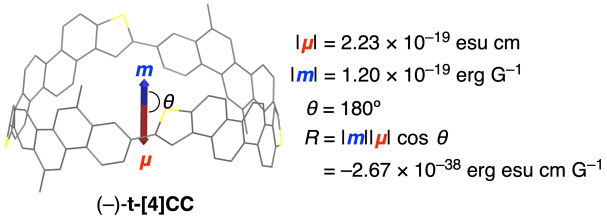

Figure 3. Physical parameters of chiroptical properties of (–)-**t-[4]CC** (B3LYP/6-31G(d,p)).

-Synthesis

We then started to synthesize the target molecule (**t-[4]CC**) (Figure 4a). For the synthesis of cylindrical cycloarylenes, Pt-mediated coupling reaction was used at the macrocyclization step.[7,8] Although this reaction is often used as homo-coupling reaction, a few examples reported cross-coupling Pt-mediated macrocyclization of bisplatinated arene and stannylated thiophene derivative.[9,10] We then transformed literature-known compounds **1** and **2** into precursors **3** and **4** respectively.[11,12] Obtained precursors **3** and **4** were mixed in *o*-dichlorobenzene (*o*DCB), and the reductive elimination from a tetrameric platinum complex by heating with excess amount of triphenylphosphine gave **t-[4]CC** in 16% yield. Depending on orientations of arylene panels, there are 5 possible diastereomers (4 enantiomeric pairs and 1 *meso* isomer) (Figure 4b).[11] Among them, a single diastereomer was selectively obtained as a racemate. By utilizing COSY and

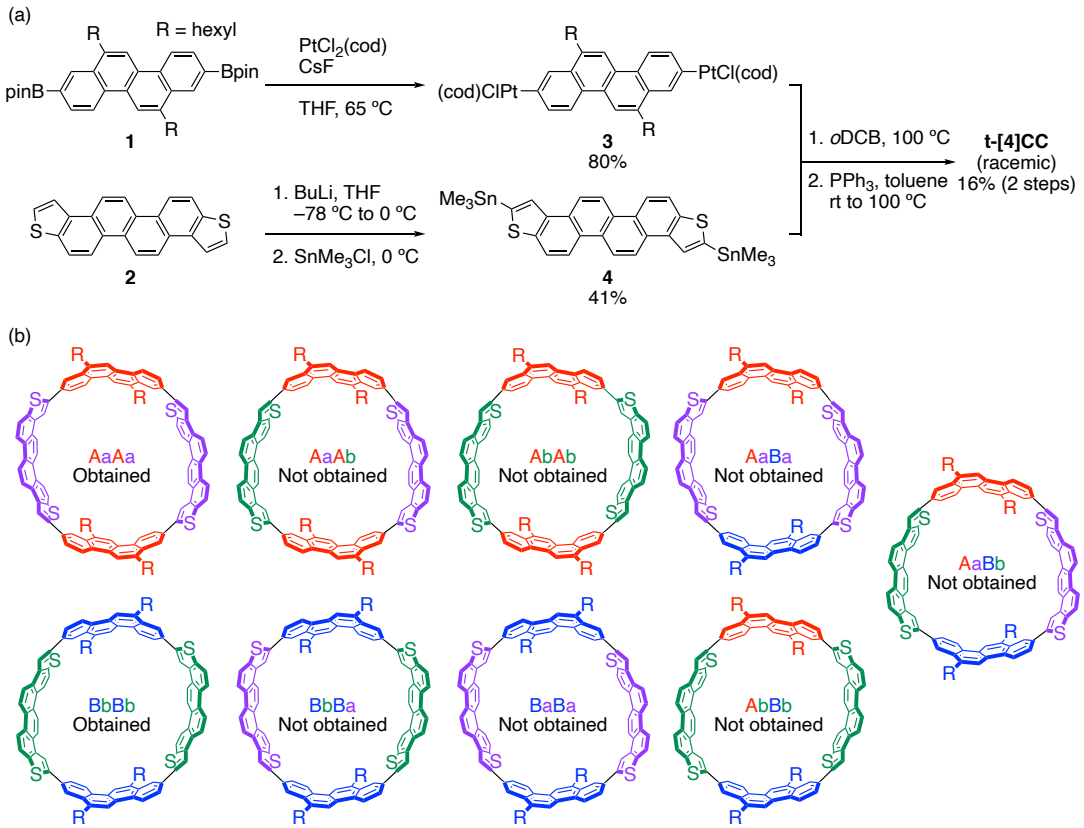

Figure 4. (a) Synthesis of **t-[4]CC**. (b) Structures of 9 possible stereoisomers of **t-[4]CC**.

ROESY, the structure of the obtained diastereomer was unambiguously determined as AaAa/BbBb isomers by indicating panel orientations as A/B for chrysenylene and a/b for thiopheno-doped chrysenylene panels.

Separation of AaAa/BbBb isomers was performed with cholesterol-loaded chiral silica gel columns (Figure 5). In the analytical HPLC chart of racemic t-[4]CC, two peaks with the opposite circular polarization were observed. These two enantiomers were successfully separated by the preparative column. The purity of separated enantiomers was confirmed by the analytical HPLC. The two enantiomers were labeled with $(-)_{380}$ and $(+)_{380}$ with the sign of CD signals at 380 nm (the retention time is 17 min and 20 min respectively). By comparing the TDDFT-simulated and experimental spectra of CD spectroscopy, the absolute configurations of $(-)_{380}$ and $(+)_{380}$-isomers were determined as AaAa and BbBb isomers, respectively.

-Chiroptical Properties

The chiroptical properties of (+)/(–)-**t-[4]CC** were investigated. First, we measured CD spectra of enantiomers were measured and obtained mirror-image spectra (Figure 6a). The experimental rotatory strength (R_{exp}) for S_0-S_1 transition was derived as -2.33×10^{-38} erg esu cm G^{-1}, which matched well with a theoretical rotatory strength (R_{calc}) of -2.67×10^{-38} erg esu cm G^{-1} from TDDFT calculations. The absolute values of R were ~6-times smaller than that of **[4]CC** (12.7×10^{-38} erg esu cm G^{-1}). This indicated that the $|\boldsymbol{\mu}|$ value could be reduced as designed. However, the experimental results of the dissymmetric factors were against our expectations (Figure 6b). Despite the theoretical predictions of $|g_{calc}| = 1.67$ for S_0-S_1 transition, the recorded value was 0.006 (422 nm). The $|g_{lum}|$ values of CPL were also measured and recorded as 0.004.

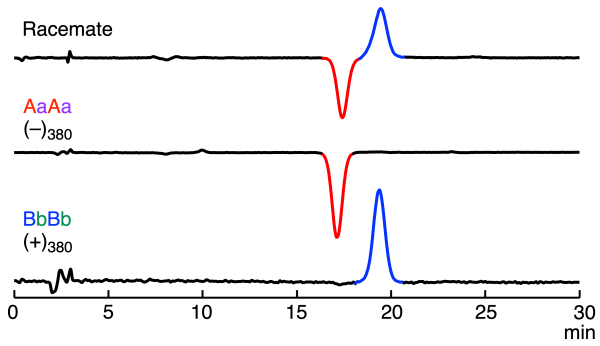

Figure 5. Chromatograms of the **t-[4]CC** racemate, (–)- and (+)-**t-[4]CC** (CD detection at 380 nm). COSMOIL Cholester was used (eluent = 40% MeOH/CH_2Cl_2, flow rate = 1.0 mL min^{-1}, 40 ºC).

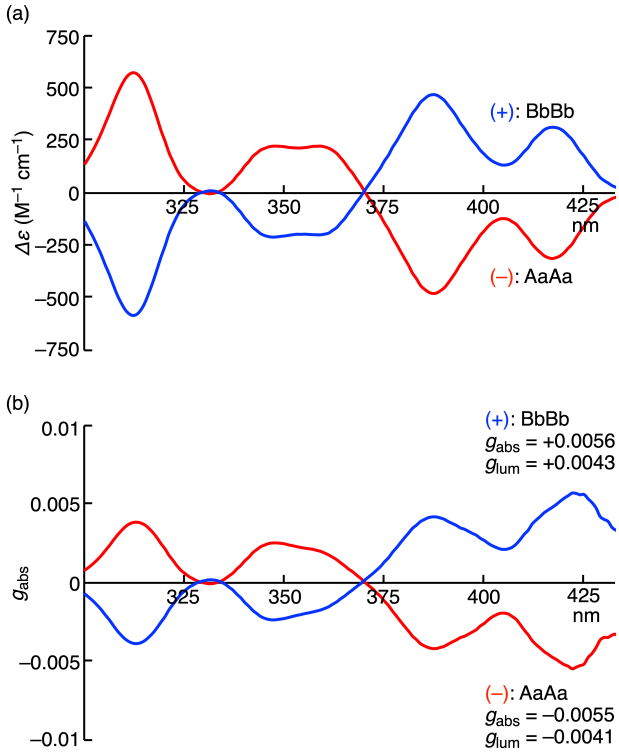

Figure 6. Chiroptical properties of (+)- and (–)-**t-[4]CC** (Solvent: toluene, concentration: 6.08×10^{-6} M for (–)-AaAa isomer and 6.48×10^{-6} M for (+)-BbBb isomer, temp.: 25 ºC). (a) CD spectra. (b) Dissymmetry factors obtained from CD and UV spectra.

-Structural Analysis

To reveal the structural origin of the small |*g*| values, we then performed the structural analysis of **t-[4]CC**. The structure of **t-[4]CC** was unambiguously disclosed by single-crystal X-ray analyses. Single crystals were obtained from a racemic mixture of **t-[4]CC**. Seen from the top side, the cylindrical structure was found to be distorted to possess an oval shape (Figure 7a), which is likely due to crystal packings. This indicated that the cylinder was easy to be affected by structural deformations. We then analyzed the structural deformations thoroughly by utilizing π-orbital axis vectors (POAVs).[13] As shown in Figure 7b, atoms at single-bond linkages were found to be most pyramidalized. Dihedral angles Φ showed deviations from an optimized structure (Φ = +23º).

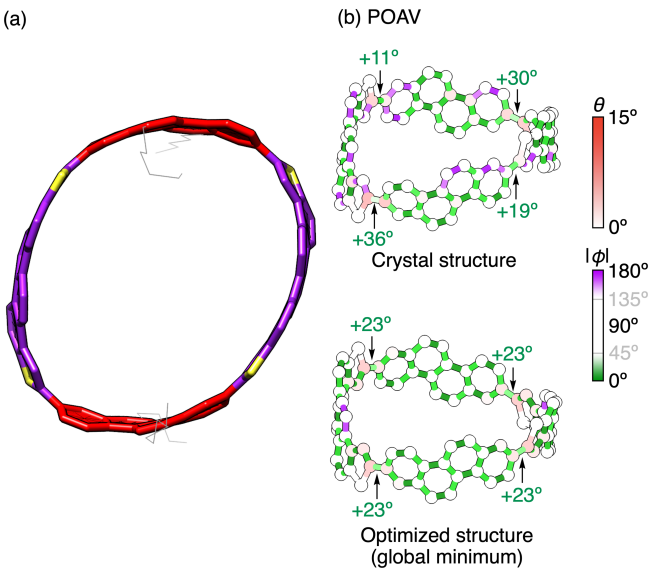

Figure 7. Molecular structures of **t-[4]CC**. (a) A crystal structure of **t-[4]CC**. A (–)-AaAa isomer is shown from the racemate. (b) POAV color mappings of pyramidalization angle and dihedral angles (Φ) for crystal and theoretical structures of AaAa isomer.

To deepen the understanding of the structure-property relationship, we investigated the effects of structural deformations on chiroptical properties with the aid of theoretical calculations. We first estimated the effects of distortions with dihedral angle (Φ) on the energy (ΔE) by twisting one biaryl linkage by ±5º for ten steps with relaxed scan calculations (Figure 8a). The estimated energy increase was subtle, which means the twisting of biaryl linkages is tolerated in the solution. With the 21 structures obtained by the scan calculations, we performed TDDFT calculations to reveal the spectral properties of every structure (Figure 8b). Although the structural change did not affect $\boldsymbol{m}$, it dramatically changed $\boldsymbol{\mu}$ and angle θ (Figure 8c). The twisting did not influence R values despite the dramatic change of $\boldsymbol{\mu}$, and the values were consistent with the R_{exp} value (Figure 8d). In contrast, the theoretical $|g_{abs}|$ value depended on the structural change

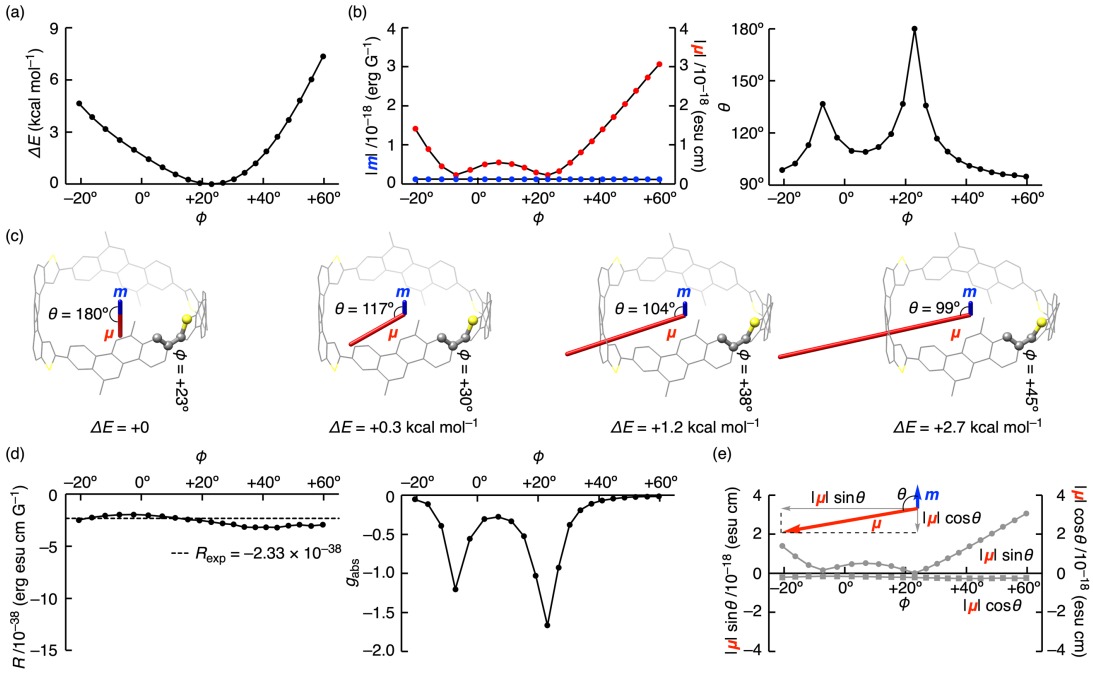

Figure 8. Effects of the twisting at one biaryl linkage on chiroptical properties of **t-[4]CC**. (a) Dependence of energies (ΔE) on Φ. (b) Dependence of $\boldsymbol{m}$, $\boldsymbol{\mu}$ and θ on Φ. (c) Representative structures from the scan calculations with Φ, ΔE, $\boldsymbol{m}$, $\boldsymbol{\mu}$ and θ. (d) Dependence of R and g_{abs} on Φ. (e) Dependence of $|\boldsymbol{\mu}|\sin\theta$ and $|\boldsymbol{\mu}|\cos\theta$ on Φ.

considerably. It can be reduced from a maximum value of 1.67 to a minimum value of 0.013 within the energy range of ΔE <8 kcal mol^{-1}. Then, through the calculations, we found that the $|g|$ value can be dramatically reduced with the Φ fluctuations of even one biaryl linkage without affecting the R value. We believe that the twisting of biaryl linkage should be taken into consideration as one of important factors in the future research.

By carefully examining the fundamental parameters, we tried to explain the Φ-dependence of R and g values reasonably. The R value is determined by $\boldsymbol{m}$, $\boldsymbol{\mu}$ and θ in the following relationship.

$$R = |\boldsymbol{m}||\boldsymbol{\mu}|\cos\theta \quad \text{eq. 2,}$$

As shown in Figures 8b and 8e, $|\boldsymbol{m}|$ and an axial component of $\boldsymbol{\mu}$ ($|\boldsymbol{\mu}|\cos\theta$) were not affected by the twisting of biaryl linkages, which can well explain the inertness of the R values. On the other hand, the formula of the g value shown as equation 1 (Figure 2b) can be rewritten as the following relationship.

$$g = \frac{4|\boldsymbol{m}||\boldsymbol{\mu}|\cos\theta}{|\boldsymbol{m}|^2 + (|\boldsymbol{\mu}|\cos\theta)^2 + (|\boldsymbol{\mu}|\sin\theta)^2} \quad \text{eq. 3,}$$

An orthogonal component of $\boldsymbol{\mu}$ ($|\boldsymbol{\mu}|\sin\theta$), which appeared in the denominator, was found to be significantly sensitive to the structural fluctuations as shown in Figure 8e. Therefore, we concluded that the sensitivity of $|\boldsymbol{\mu}|\sin\theta$ is the origin of the discrepancy between the experimental and theoretical $|g|$ values.

-Application to Thin-film Transistor

Since precursor **2** (**ChDT–α**)[12] is a fascinating p-type organic semiconducting material due to its unique HOMO shape, the property of **t-[4]CC** as organic semiconductor was investigated. As shown in Figure 9, theoretical calculation based on the crystal structure revealed that the transfer integral values of some dimers are around 10 meV. Therefore, it seems possible to occur the carrier transport in particular directions, for instance, between *a*-axis and *c*-axis in this crystal structure. To examine the possibility that **t-[4]CC** can be applied to thin film transistors, the fabrication of **t-[4]CC** thin film was tried using edge-casting method[14] and gap-casting method[15]. This trial provided films which were not crystalline but like amorphous. Further condition examinations are needed to obtain crystalline films of **t-[4]CC**, which could be applicable to thin film transistors as predicted by theoretical calculations.

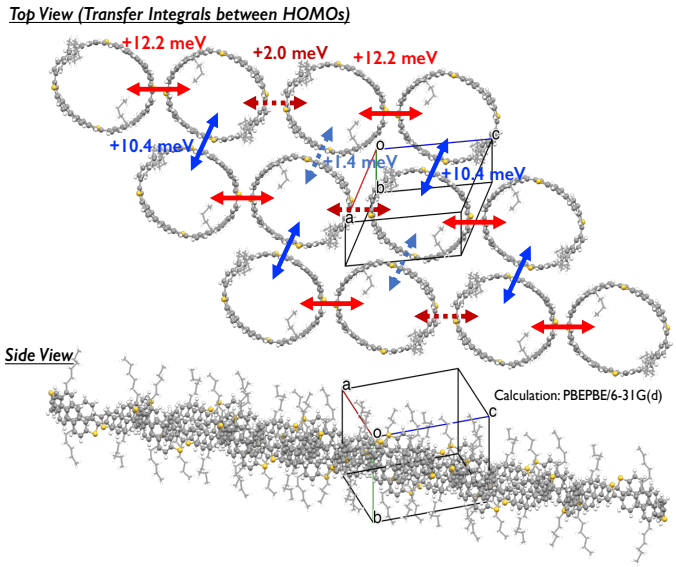

Figure 9. Transfer integral values of dimers in the **t-[4]CC** crystal structure (calculated at PBEPBE/6-31G(d)).

Summary

In summary, we explored the manipulation of chiroptical properties in nanotube molecules by a desymmetrization strategy with sulfur doping. The total $\boldsymbol{\mu}$ was arranged to achieve an ideal relationship of $|\boldsymbol{m}|\sim|\boldsymbol{\mu}|$ for maximizing the dissymmetry factor $|g|$. The designed molecule, **t-[4]CC**, was synthesized by stereoselective cross-coupling reaction of doped and undoped arene panels. The chemical structure was unambiguously disclosed and the enantiomers were successfully separated. However, the observed $|g|$ values were much smaller than the theoretical values. The analysis of the discrepancy by theoretical calculations showed that the $|g|$ values were sensitive to the twisting of biaryl linkages in the solution. These results suggested that the rigidity of the cylinder could be necessary for enhancing the dissymmetry factor. We also tried the examination of the properties as an organic semiconducting material by the theoretical calculation based on **t-[4]CC**'s crystal structure and the fabrication of its thin-film. We believe that this study will help accelerate the development of CPL materials and organic semiconducting materials.

Some results of this report have been published in Angewandte Chemie International Edition.[16]

Acknowledgement

We would like to show our greatest appreciation to Profs. T. Okamoto and H. Isobe for all their support. We would also thank Prof. T. Tsukuda and Prof. K. Nozaki for their advice and approval of our proposal. We appreciate KEK Photon Factory (no. 2020G504) for the use of X-ray diffraction instruments and Hiroshima University (Profs. R. Sekiya, T. Haino and T. Takata) for the CPL instruments. We are grateful to MERIT program for providing us an opportunity for the self-directed joint research.

References

[1] (a) Biot, J. B. *Mém. Acad. Sci.* **1835**, *13*, 39-175. (b) Pasteur, L. *C. R. Séances Acad. Sci.* **1848**, *26*, 535-538. (c) Pasteur, L. *Ann. Chim. Phys.* **1848**, *24*, 442-459. (d) Pasteur, L. *Ann. Chim. Phys.* **1850**, *28*, 56-99.

[2] Gal, J. *Helv. Chim. Acta* **2013**, *96*, 1617-1657.

[3] Sánchez-Carnerero, E. M.; Agarrabeitia, A. R.; Moreno, F.; Maroto, B. L.; Muller, G.; Ortiz, M. J.; de la Moya, S. *Chem. –Eur. J.* **2015**, *21*, 13488-13500.

[4] (a) Sato, S.; Yoshii, A.; Takahashi, S.; Furumi, S.; Takeuchi, M.; Isobe, H. *Proc. Natl. Acad. Sci. U.S.A.* **2017**, *114*, 13097-13101. (b) Sato, S.; Yoshii, A.; Takahashi, S.; Furumi, S.; Takeuchi, M.; Isobe, H. *Proc. Natl. Acad. Sci. U.S.A.* **2019**, *116*, 5194-5195.

[5] Kogashi, K.; Matsuno, T.; Sato, S.; Isobe, H. *Angew. Chem., Int. Ed.* **2019**, *58*, 7385-7389.

[6] Lu, T.; Chen, F. *J. Comput. Chem.* **2012**, *33*, 580-592.

[7] Zhang, F.; Götz, G.; Winkler, H. D. F.; Schalley, C. A.; Bäuerle, P. *Angew. Chem., Int. Ed.* **2009**, *48*, 6632-6635.

[8] Yamago, S.; Watanabe, Y.; Iwamoto, T. *Angew. Chem., Int. Ed.* **2010**, 49, 757-759.

[9] Ball, M.; Fowler, B.; Li, P.; Joyce, L. A.; Li, F.; Liu, T.; Paley, D.; Zhong, Y.; Li, H.; Xiao, S.; Ng, F.; Steigerwald, M. L.; Nuckolls, C. *J. Am. Chem. Soc.* **2015**, *137*, 9982-9987.

[10] Ball, M. L.; Zhang, B.; Xu, Q.; Paley, D. W.; Ritter, V. C.; Ng, F.; Steigerwald, M. L.; Nuckolls, C. *J. Am. Chem. Soc.* **2018**, *140*, 10135-10139.

[11] Hitosugi, S.; Nakanishi, W.; Yamasaki, T.; Isobe, H. *Nat. Commun.* **2011**, *2*, 492.

[12] Yamamoto, A.; Murata, Y.; Mitsui, C.; Ishii, H.; Yamagishi, M.; Yano, M.; Sato, H.; Yamano, A.; Takeya, J.; Okamoto, T. *Adv. Sci.* **2018**, *5*, 1700317.

[13] (a) Haddon, R. C. *Acc. Chem. Res.* **1988**, *21*, 243-249. (b) Haddon, R. C. *J. Phys. Chem. A* **2001**, *105*, 4164-4165. (c) Mio, T.; Ikemoto, K.; Isobe, H. *Chem. Asian J.* **2020**, *15*, 1355-1359.

[14] Uemura, T.; Hirose, Y.; Uno, M.; Takimiya, K.; Takeya, J. *Appl. Phys. Express* **2009**, *2*, 111501.

[15] Soeda, J.; Uemura, T.; Mizuno, Y.; Nakao, A.; Nakazawa, Y.; Facchetti, A.; Takeya, J. *Adv. Mater.* **2011**, *23*, 3681.

[16] Fukunaga, T. M.; Sawabe, C.; Matsuno, T.; Takeya, J.; Okamoto, T.; Isobe, H. *Angew. Chem., Int. Ed.* Published online (doi: 10.1002/anie.202106992).